Regional Distribution of Glycogen in the Mouse Brain Visualized by Immunohistochemistry

Yuki Oe, Sonam Akther, and Hajime Hirase

Abstract Considering that the brain constantly consumes a substantial amount of energy, the nature of its energy reserve is an important issue. Although the brain is rich in lipid content encompassing membranes, myelin sheath, and astrocytic lipid droplets, it is devoid of adipose tissue which serves as an energy reserve. Notably, glycogen represents the major energy store in the brain. While glycogen has been observed mainly in astrocytes for decades by electron microscopy, glycogen distribution in the brain has only been partially documented. The involvement of glycogen metabolism in memory consolidation, demonstrated by several research groups, has reiterated the functional significance of this macromolecule and the need for description of its comprehensive distribution in the brain. The combination of focused microwave-assisted brain fixation and glycogen immunohistochemistry permits assessment of glycogen distribution in the rodent brain. In this article, we describe glycogen distribution in the mouse brain using glycogen immunohistochemistry. We find heterogeneous glycogen storage patterns at multiple spatial scales. The heterogeneous glycogen distribution patterns may underlie local energy metabolism or synaptic activity, and its mechanistic understanding should extend our knowledge on brain metabolism in health and disease.

Keywords Glycogen immunohistochemistry · Forebrain · Olfactory bulb · Hippocampus · Cortex · Striatum

Y. Oe (✉)
RIKEN Center for Brain Science, Wako, Saitama, Japan
e-mail: yuki.oe@riken.jp

S. Akther · H. Hirase (✉)
RIKEN Center for Brain Science, Wako, Saitama, Japan

Saitama University Brain Science Institute, Saitama, Japan
e-mail: hajime.hirase@riken.jp

M. DiNuzzo, A. Schousboe (eds.), *Brain Glycogen Metabolism*, Advances in Neurobiology 23, https://doi.org/10.1007/978-3-030-27480-1_5

1 Introduction

The energy consumption of the brain is exceptionally high compared to other organs (Raichle and Gusnard 2002). The fundamental energy substrate—adenosine triphosphate (ATP)—is primarily derived from glucose that is supplied by blood circulation in the brain. According to the astrocyte-to-neuron lactate shuttle hypothesis, glucose from blood circulation is transported to astrocytes and broken down into lactate which, in turn, is shuttled to neighboring neuronal compartments. Inside neurons, lactate is converted into pyruvate and further metabolized by the tricarboxylic acid (TCA) cycle to produce ATP molecules. As in other peripheral organs such as the liver or muscles, a portion of glucose is stored primarily inside astrocytes in the form of glycogen. While described in detail in other chapters of the present volume, brain glycogen metabolism supports: (1) on-demand supply of increased energy and (2) promotion of long-term synaptic plasticity. The degrees to which these functionalities are recruited have not been explicitly described and they likely depend on brain region and state. However, the examination of glycogen distribution will enable us to assess the capacity of astrocytes to execute such functions in distinct brain regions.

There are several ways to determine brain glycogen distribution. First, brain regions of interest can be dissected and biochemical assays can be performed on them. Quantitative biochemical glycogen assays include phenol sulfuric acid and OxiRed fluorescent probe methods which react with the amount of (oxidized) glucose generated by enzymatic breakdown of glycogen. The signal strength reflects the amount of glycosyl units that constitute glycogen molecules in the sample. Although these biochemical methods are quantitative, they require a considerable amount of sample and hence are not suitable for assessing the spatial distribution of glycogen finer than broad brain regions. For instance, the BioVision glycogen assay kit K646–100 recommends 10 mg of tissue. Considering the low glycogen content in the brain (an order of magnitude smaller than the liver or skeletal muscle content of a few 100 μM/g wet tissue), a larger sample amount warrants accurate measurements. Since a mouse brain weighs only about half a gram, dissection and biochemical assay should be performed with great care. In the past, glycogen quantification has been performed with the rat brain which typically weighs over 2 g.

Second, glycogen granules are observed as electron-dense puncta in lead- or osmium-intensified sections by electron microscopy. Therefore, electron microscopy provides a direct assessment of subcellular distribution of glycogen. However, electron microscopy is limited by the size of observable area, which is typically in the range of several micrometers in horizontal dimensions of a thickness of tens of nanometers. Even with the development of serial block-face scanning electron microscopy or automated serial microscopy with ultrathin sections mounted on tapes, the volume is practically limited to a single cortical column. The small volume of observation makes approaches with electron microscopy unrealistic to assess brain-wide glycogen distribution.

Third, nuclear magnetic resonance spectroscopy (MRS) is a method that detects unique resonance frequencies glycogen molecules in a magnetic field. The advantage of MRS is that this method is quantitative and can be readily performed on live subjects. For example, liver and skeletal muscle glycogen levels have been quantified by MRS in human subjects (Cline et al. 1999; Magnusson et al. 1992; Öz et al. 2003). However, MRS is limited by its spatial resolution. Since the brain stores an order of magnitude lower amount of glycogen than the liver or skeletal muscles, a typical voxel used to assess glycogen content is larger than a centimeter in each dimension and requires the summation of scans for extended periods of time to obtain reliable signals (Öz et al. 2007). While this method can possibly address glycogen distribution of a human brain with the coarse resolution, it is not suitable for characterizing the glycogen distribution of individual brain regions or brains of smaller animals.

Fourth, compared with the above methods, histological examination by light microscopy is a suitable approach to characterize the regional, cellular, and subcellular distribution of glycogen. A critical point to consider for the histological approach is how specific glycogen is labeled in brain sections. Glycogen has traditionally been stained by the periodic acid-Schiff (PAS) histochemical staining procedure, particularly for clinical research purposes. PAS staining is used to indicate glycogen in liver samples where hepatocytes store high amounts of glycogen. However, PAS staining also labels glycoproteins and proteoglycans which are abundant in the brain. Therefore, PAS staining is not ideal for the evaluation of brain glycogen distribution in terms of specificity. Immunohistochemistry is a method which achieves relatively high specificity, given a specific primary antibody. Additionally, immunohistochemistry permits labeling of secondary or tertiary molecules which are useful in determining cell types that store glycogen. In this chapter, we describe brain glycogen distribution using two monoclonal antibodies against glycogen.

After describing the procedure for glycogen immunohistochemistry, we describe brain glycogen distribution at three levels: (1) macroscopic distribution by distinct brain region, (2) microscopic (subcellular) distribution within astrocytes, the principal glycogen storage cell type, and (3) mesoscopic distribution in brain areas of high glycogen content.

2 Glycogen Immunohistochemistry

Glycogen is a storage of glucose and its size varies dynamically according to usage or storage of glucosyl units. For instance, when the tissue oxygen level is low, cell energy metabolism shifts to anaerobic metabolism whereby glycogen is broken down into glucose-1-phosphate molecules. Likewise, when excess glucose is available, glycogenesis occurs in cells specialized to store glycogen including hepatocytes, myocytes, and in the central nervous system, astrocytes. Brain glycogen has also been reported to be consumed during prolonged aerobic exercise (Matsui et al. 2011).

Brain immunohistochemistry is typically performed on perfusion-fixed tissue. Perfusion fixation is generally performed in two steps: transcardial perfusion with physiological solution (e.g., saline, phosphate buffered saline, Ringer's solution, etc.), followed by transcardial perfusion of fixative (e.g., 4% paraformaldehyde in 0.1 M phosphate buffer). While the purpose of the first step is to remove blood from the brain, this step typically lasts for a few minutes or longer, which inevitably puts the brain under an anoxic state. As a result, glycogen is vastly degraded and little glycogen remains in the perfusion-fixed brain. A possible way to prepare a fixed brain sample without perfusion is to fix an acutely prepared alive brain slice. Acute brain slice preparation is a common procedure practiced in *in vitro* electrophysiology laboratories and slices are usually recovered in oxygenated artificial cerebral spinal fluid for an hour or so before experiments. Indeed, it has been shown that glycogen in hippocampal acute slices is emptied immediately after slice preparation already (Fiala et al. 2003; Takano et al. 2014). Brain dissection and slice cutting surely induce trauma and resultant extracellular potassium elevation. High extracellular potassium has previously demonstrated to trigger glycogenolysis via activation of soluble adenylyl cyclase (Choi et al. 2012).

Because glycogen is very sensitive to brain insult, a method that instantly preserves the *in vivo* state of metabolism is essential for proper histological visualization of glycogen. Rapid freezing of the brain in liquid nitrogen is a common procedure for biochemistry and in situ hybridization. Focused microwave irradiation is another procedure practiced in biochemical investigation of brain metabolism or protein phosphorylation. The former approach aims to preserve the metabolic state of the brain by halting enzymatic activity by lowering the temperature, whereas the latter approach denatures and inactivates metabolic enzymes by instantaneously heating the sample to 80–90 °C.

Previous biochemical examinations of brain glycogen showed that microwaved preparations preserve significantly higher amounts of glycogen (> ~twice) than rapid freezing (Sagar et al. 1987). More recently, Sugiura et al. (2014) compared the abundance of metabolic substrates in hippocampal samples prepared by post-euthanasia whole-brain freezing, in situ freezing, or focused microwave irradiation. Accordingly, they found that focused microwave irradiated samples contained higher amounts of ATP, adenosine diphosphate (ADP) and pyruvate compared with the other methods, which had more degraded purine and lactate levels. This result shows that focused microwave irradiation preserves the aerobic respiratory state of the brain (which is the default *in vivo* respiration mode) and is adequate for glycogen immunohistochemistry.

While brain samples prepared by focused microwave irradiation have been used for biochemical evaluation of glycogen content (Sagar et al. 1987) and PAS staining (Kong et al. 2002), glycogen immunohistochemistry has not been performed until recently. Here we summarize the glycogen immunohistochemistry procedures used in our laboratory. Currently, two mouse monoclonal IgM antibodies have been verified to be suitable for glycogen immunohistochemistry (Fig. 1). The ESG1A9 antibody (ESG) is raised against enzymatically synthetized glycogen (hence the name ESG), and it tends to have higher affinity to large glycogen molecules (Nakamura-Tsuruta et al. 2012). The IV58B6 antibody (IV) has affinity for glycogen

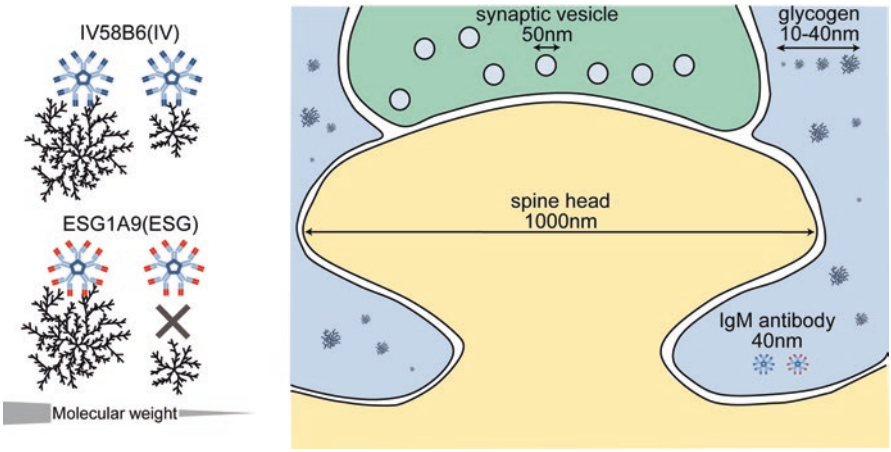

Fig. 1 Consideration of spatial scales in glycogen immunohistochemistry. Left panel: The IV58B6 antibody is considered to have an affinity for glycogen of all sizes, whereas the ESG1A9 antibody has an affinity for large glycogen macromolecules. Right panel: Sketch of a synapse and perisynaptic astrocytic processes incorporating realistic spatial scales

of all sizes (Baba 1993). The exact manner in which these two antibodies express the differential affinity patterns has not been identified. It is supposed that enzymatically synthesized glycogen has a different branching pattern from that of natural glycogen, and the epitopes are associated with the branching pattern.

Adult mice are euthanized by focused microwave irradiation using a MMW-05 microwave fixation system (Muromachi Kikai, Tokyo, Japan). Considering circadian modulation of astrocytic and metabolic functions, it is a reasonable idea to sacrifice mice in a defined time of the day. For instance, all mice studied in our recent study were sacrificed between 6:00 and 8:00 p.m., i.e., within 2 h before the end of diurnal period (Oe et al. 2016). Briefly, a mouse was confined in a specialized tubular animal holder with a hollow wall filled with water (WJM-24 or WJM-28, Muromachi Kikai). The holder with the animal is then placed inside MMW-05. High-energy microwave (5 kW) was focused at the head of the mouse for 0.94–1.05 s. Immediately after focused microwave euthanasia, the brain was removed from the skull and immersed in fixative (4% paraformaldehyde in 0.1 M phosphate buffer) for overnight at 4 °C.

Brain sections of 60 μm thickness were prepared in PB using a microslicer (Pro-7 Linear Slicer, DSK, Japan). After washing in phosphate buffered saline (PBS), the sections were incubated in PBS containing 0.1% Triton X-100 and primary antibodies for 24 hours at 4 °C while gently shaking. The concentrations of ESG and IV antibodies are 1:50 (15 μg/ml) and 1:300 (30 μg/ml), respectively. As mentioned previously, both ESG and IV antibodies are IgM which are several times larger than IgG in molecular size. Therefore, penetration of the primary antibodies should be performed extensively. The authors are not aware of an IgG antibody for glycogen that can be used for immunohistochemistry at this time. The sections were then

washed three to five times in Tris-buffered saline and incubated with fluorescent secondary antibodies (1:1000 in PBS containing 0.1% Triton X-100, Alexa Fluor 488 or 594, Life Technologies). Brain slices were mounted on slide glasses and coverslipped with PermaFluor mounting medium (Thermo Scientific).

3 Glycogen Distribution in Major Brain Regions

Based on the immunohistochemistry protocol described in the previous section, glycogen distribution was visualized in coronal and sagittal sections of the mouse brain. These preparations allow the evaluation of glycogen distribution in macroscopic scales. As shown in examples in Fig. 2, the IV (pan-glycogen) antibody labels the brain fairly extensively with regional heterogeneity. For example, the hippocampus generally has high-intensity signals while the principal cell body layers of the hippocampus are low in signal intensities. Moreover, the white matter has been found to be generally low in signal intensity. Accordingly, the corpus callosum, hippocampal fimbria-fornix, medial forebrain bundle, and arbor vitae of the cerebellum are distinguished as low-intensity structures. Moreover, stripe patterns

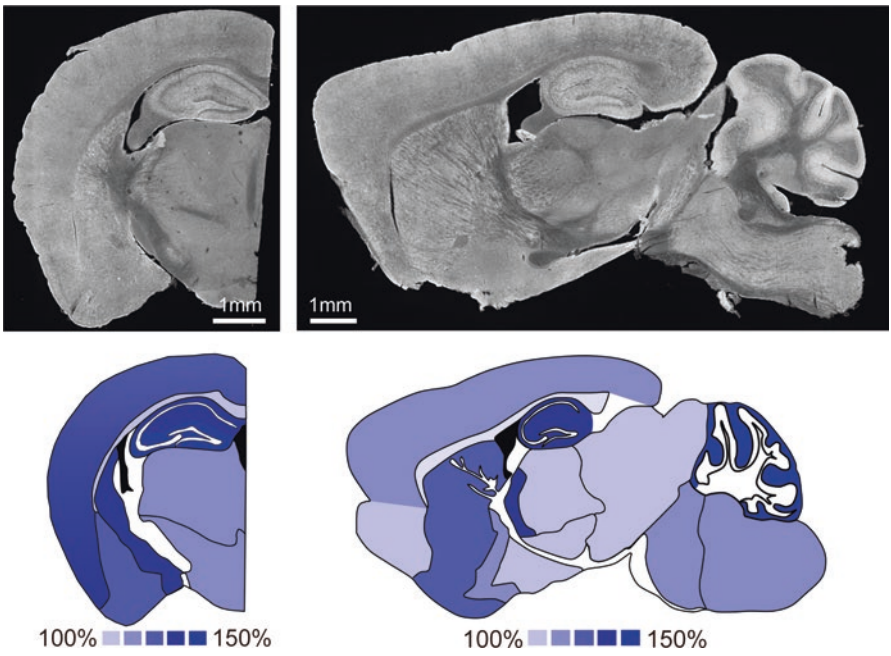

Fig. 2 Glycogen immunohistochemistry on microwave-fixed mouse brain at microscopic scale using IV58B6. Upper panel: Examples of glycogen immunohistochemistry of coronal (left) and sagittal (right) sections. Lower panel: Relative glycogen immunohistochemical signal averaged over 9 mice. Reproduced from Oe et al. (2016)

of axon bundles labeled in low intensity are apparent in sagittal sections of the striatum. Amongst major gray matter structures, the cerebellar cortex, hippocampus, thalamic reticular nucleus, striatum, globus pallidus, substantia nigra (pars reticulata), and pons are labelled well with IV. On the other hand, subcortical structures including the dorsal thalamus and hypothalamus generally were found to be low in IV signals.

The ESG antibody labels the brain rather modestly and signals are barely discernible from intrinsic fluorescence in many brain areas where green-fluorescent secondary antibody is used for visualization. However, where signals were found high with the IV antibody, ESG signals are also detected with high intensity. For instance, ESG signals are easily detected in the hippocampus, striatum and enriched in some parts of allocortex (e.g., entorhinal, perirhinal, and olfactory cortices). In the neocortex and cerebellar cortex, sparse labeling patterns on superficial layers are observed. We note that substantia nigra pars reticulata and ventral tegmental area, the two main dopaminergic brain areas, are labeled in high intensities.

It is imperative to verify the signal strength of microwave fixation-assisted glycogen immunohistochemistry with the actual glycogen content. To this end, we have measured the glycogen contents in the microwave-treated cortex, striatum, hippocampus and cerebellum using a biochemical assay kit (K646–100, BioVision). As a result, we found a reasonable correspondence between glycogen content and relative immunohistochemical signal, except for the cerebellum (Oe et al. 2016). The cerebellar glycogen content was measured to be lower than relative immunohistochemical signals, most likely because the biochemical cerebellar samples included a large proportion of the white matter (arbor vitae) compared with other forebrain structures. Multiple studies have addressed glycogen content by brain region using biochemical assays on microwave fixed samples. We have rearranged published results from rats (Kong et al. 2002; Matsui et al. 2011; Sagar et al. 1987) and mice (Oe et al. 2016) in Fig. 3. These results agree well and the mouse glycogen immunohistochemistry data show that the hippocampus, cerebellum, and the cortex store relatively high levels of glycogen. Interestingly, striatal glycogen is found to be relatively low in both studies, which differs from our mouse study. It is possible that species differences exist in the storage and usage of glycogen. Additionally, regional glycogen storage may depend on metabolic states of the brain, including sleep cycle and circadian rhythm.

4 Astrocytes Store Glycogen in the Forebrain

The forebrain is the most recently developed division of the vertebrate brain and is responsible for higher order functions, such as perception, memory, and most likely, consciousness. The forebrain includes cortical structures and the basal forebrain, basal ganglia, thalamus, and hypothalamus. While there are regional variabilities in glycogen storage within the forebrain, glycogen signals are predominantly found in astrocytes in all areas of the forebrain. As such, IV glycogen immunohistochemistry results in astrocytic patterns. Neurons and microglia are predominantly devoid of IV

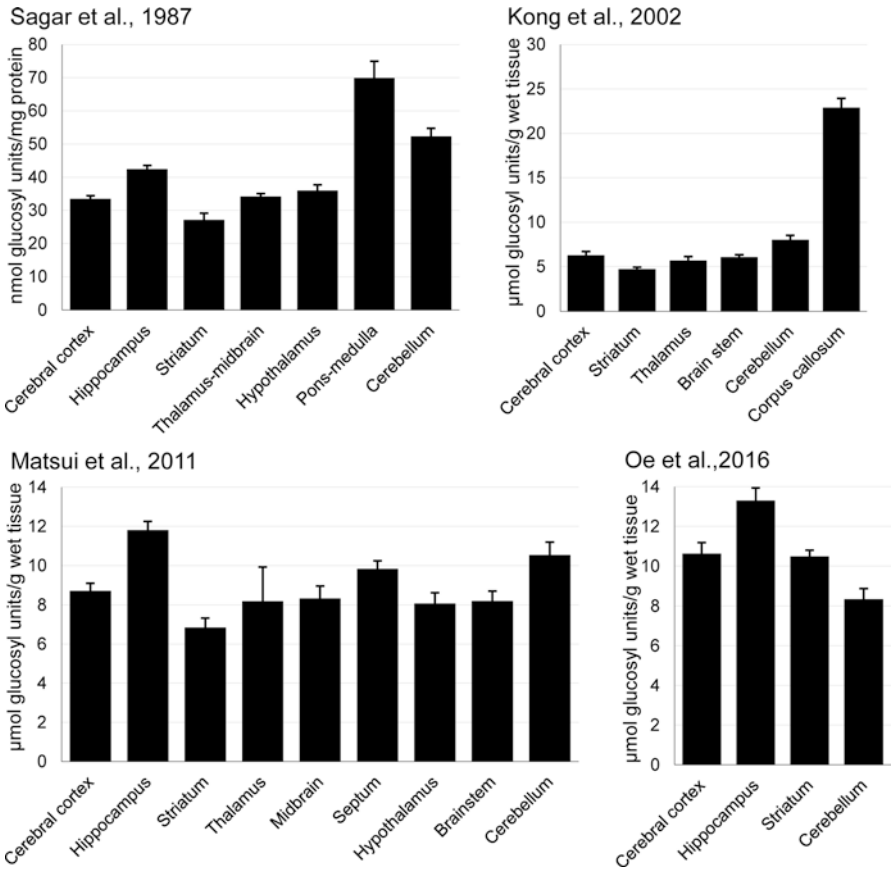

Fig. 3 Biochemical assessment of glycogen content by major brain region. Four published studies are presented. These measurements are made using microwave-fixed brains. Measurements are from rats for Sagar et al. (1987), Kong et al. (2002), and Matsui et al. (2011) while measurements by Oe et al. are from mice. Bar graph are replotted from respective original publications with bar orders modified for comparison purposes

signals. Astrocytic IV signals are characterized by high-intensity and dense punctate patterns (Fig. 4). Less intense and relatively smooth signals are observable in astrocytic cytosol in between IV puncta. By contrast, ESG signals are exclusively punctate and there is hardly any discernible signals outside puncta (Oe et al. 2016). Whether the punctate patterns labeled by IV and ESG overlap has not been addressed; however, these punctate patterns are emphasized in astrocytic microprocesses (Fig. 4a) and endfeet (Fig. 4b), rather than somata or primary branches. The distinct punctate distribution pattern supports the supposed role of glycogen as intermediate energy storage and the source of lactate for long-term synaptic plasticity. Moreover, enriched accumulation of glycogen in perisynaptic microprocesses and endfeet has been confirmed by a recent study using serial block-face scanning electron microscopy (Calì et al. 2016).

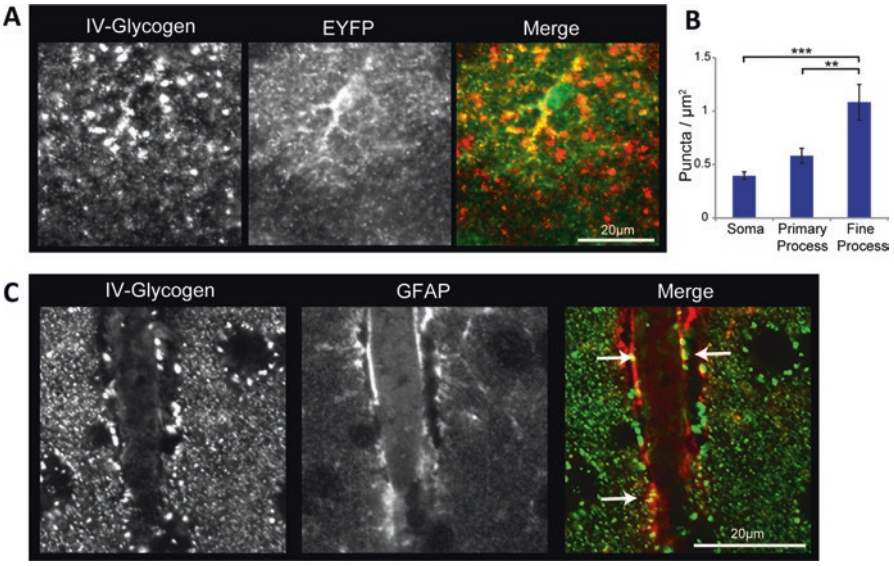

Fig. 4 Glycogen distribution in the cerebral cortex gray matter of the mouse. (**a**) Double immunohistochemistry showing IV glycogen antibody-labeling and YFP-labeled single astrocyte morphology. IV glycogen immunohistochemistry shows that glycogen is preferentially localized in fine processes of astrocytes. (**b**) Quantification of immunolabeled puncta shows preferential localization of glycogen in fine process of astrocytes. (**c**) Perivascular glycogen distribution. Large and intense glycogen puncta are observable along the vasculature. GFAP immunohistochemistry labels astrocytic endfeet which delineate the vasculature. Arrows indicate large and intense glycogen puncta that overlap with GFAP signal. Reproduced from Oe et al. (2016). GFAP: glial fibrillary acidic protein

Glycogen macromolecules are known to be organized in multiple levels of complexity; beta particles which are essentially single-core glycogen molecules, and alpha particles which are an aggregation of multiple glycogen molecules. Each beta particle has a dimer of glycogenin as the core where glycogen chains are originated. Beta particles have a maximum diameter of ~50 nm when glucose is fully stored, whereas alpha particles can be as large as a few hundred nanometers and observable in the liver (for concise reviews, Obel et al. 2012; Prats et al. 2018). Interestingly, a recent report showed that glycogenin is not a requirement of glycogen particle formation and paradoxically, glycogenin deficiency results in higher glycogen accumulation with larger particles (Testoni et al. 2017). It remains unknown if all brain glycogen particles are strictly associated with glycogenin.

An important point to consider is that both ESG and IV antibodies are IgM type and hence have a diameter of 40 nm, a size similar to a medium-size beta glycogen particle (Fig. 2). Puncta signals obtained by glycogen immunohistochemistry has aggregated appearances hinting at the existence of beta particle aggregates. Indeed classical papers by Phelps and Koizumi exemplify astrocytic glycogen particle aggregates in their electronmicrographs (Koizumi 1974; Phelps 1972). Whether such aggregates qualify to be

alpha particles is an open question. It is further tempting to speculate that the epitope for the ESG antibody is somewhat associated with a conformation of beta particle aggregates. Further structural studies are required to reveal the true nature of antibody affinity.

Classical electron microscopy studies have additionally identified electron-dense glycogen granules in pericytes, which are scaffold cells of cerebral capillaries and venules (Cataldo and Broadwell 1986). IV glycogen immunohistochemistry shows strong condensation of particles around blood vessels (Fig. 4b). A majority of perivascular glycogen signals are co-localized with GFAP-positive processes, indicating astrocytic endfeet. Co-registration of electron microscopy and ^{13}C-labeled glucose by ultra-high spatial resolution ion microprobe imaging (NanoSIMS) showed incorporation of glucose to glycogen in endfeet and other parts of astrocytes (Takado et al. 2015), though the amount of de novo glucosyl unit incorporation is 25 times smaller than that of hepatocytes in fasted mice. Additionally, there are scattered perivascular signals, which may be of pericyte origin. Pericytic glycogen distribution has not been characterized in detail, possibly because there is not an antibody that uniquely labels the morphology of pericytes. Fortunately, the proteoglycan NG2 promoter-driven transgenic mouse expresses DsRed in both oligodendrocyte precursor cells (so-called NG2-positive glia) and pericytes (Zhu et al. 2007). Future studies should be able to address pericytic glycogen distribution with this mouse strain.

5 Glycogen Distribution in Distinct Mouse Brain Regions

5.1 Cerebral Cortex

As stated previously, the total amount of cerebral cortical glycogen is relatively high compared with diencephalic structures such as the thalamus and hypothalamus. Moreover, large glycogen puncta are observable by ESG glycogen immunohistochemistry. Generally, the temporal lobe accumulates higher amounts of glycogen than other lobes. Within the temporal lobe, the piriform cortex stands out in glycogen content. Outside the temporal lobe, glycogen levels are modestly rich and regional variability across different areas of the cortex is modest.

A common characteristic of cortical glycogen distribution is layer dependency. Generally, superficial layers accumulate more glycogen than deep layers. In particular, layer 1 shows the most intense glycogen immunohistochemistry signal with large glycogen puncta which are also labeled by the ESG antibody (Fig. 5a). This may be related to the fact that synapse density is the highest in layer 1 and decreases with depth in the barrel cortex of developed mice (Chandrasekaran et al. 2015), in particular the synapse density of asymmetrical (excitatory) synapses (DeFelipe et al. 2002). Similarly, glycogen signal decreases with cortical depth and is the lowest in layer 6 (Fig. 5b), where the lowest synapse density within the cortical

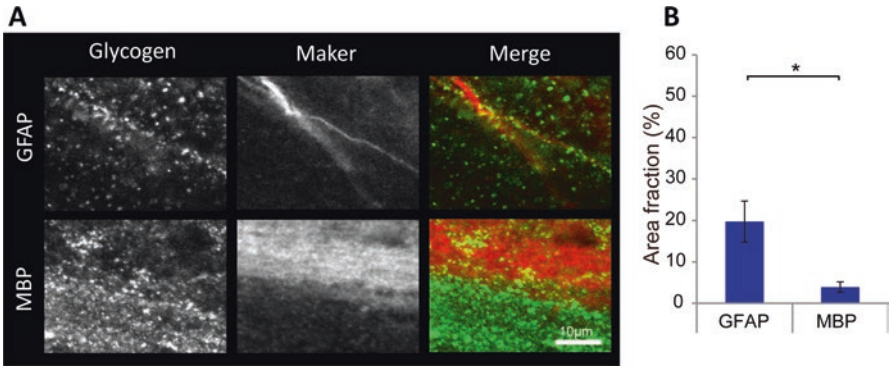

Fig. 5 Glycogen distribution in the cerebral cortex white matter. (**a**) In the upper panel, the corpus callosum is immunolabeled for glycogen (IV) and GFAP. Glycogen puncta are observed along the GFAP positive structure, suggesting astrocytic localization of glycogen. The lower panel represents the corpus callosum/alveus and hippocampal gray matter border. Strong myelin basic protein (MBP, oligodendrocyte marker) signals are seen in the cortical white matter, where glycogen signals are generally low. (**b**) Quantification of glycogen puncta by confocal microscopy indicates a preferential localization in astrocytes to oligodendrocytes (reproduced from Oe et al. (2016))

parenchyma has been reported (Chandrasekaran et al. 2015; DeFelipe et al. 2002; Schuz and Palm 1989). The positive correlation between glycogen storage and synapse density supports the idea that neuronal synapses are the consumers of glycogen metabolites (e.g., lactate). It is imperative to note however, that the synaptic organization of the mouse neocortex is considerably different from that of the rat or the human (Anton-Sanchez et al. 2014; DeFelipe et al. 2002; Palomero-Gallagher and Zilles 2017). Likewise, the periallocortex (e.g. entorhinal cortex) may have a different profile due to its distinct synaptic organization.

A natural question that arises is if the layer-dependent glycogen storage reflects the metabolic rate of a given layer. In an attempt to seek the relationship between constitutive metabolic activity and cortical layer, aerobic metabolism capability was visualized by cytochrome-c oxidase staining. Cytochrome-c oxidase signals are classically known to be obtained where energy demand is supposedly high, such as in visual areas projected from the intact eye after monocular deprivation (Wong-Riley 1979) and in layer 4 barrels of the whisker somatosensory cortex (Wong-Riley and Welt 1980). Comparison of cytochrome-c oxidase and glycogen signals in consecutive cortex sections, however, did not appear to be closely related. Rather, glycogen signals appeared relatively independent of cytochrome-c oxidase signals (Oe et al. 2016). For instance, the barrel structures were hardly discernible from IV glycogen immunohistochemistry. Therefore, it is reasonable to postulate that *constitutive* metabolic activity in the cortex might not rely heavily on glycogenolysis and is supported by glucose supply that comes from the dense network of blood circulation. Nevertheless, it is noted that *evoked* intense neuronal activity by sensory stimulation leads to local glycogenolysis in the corresponding somatosensory area, as shown by ^{14}C(3,4)glucose autoradiography (Swanson et al. 1992). One model that has gained experimental support is that glycogenolysis, and the resultant metabolite shuttle to

nearby synapses, is a key mediator of synaptic plasticity and learning (Gibbs et al. 2006; Newman et al. 2011; Suzuki et al. 2011; Wang et al. 2017). According to this view, glycogen is consumed in an on-demand manner and can be regarded as a reserve metabolite storage rather than constant supply of energy substrate.

Relatively large immunolabeled puncta (>0.5 μm diameter) are observable with the ESG antibody, especially in superficial layers. Large ESG puncta are distributed in a pattern with relatively busy clusters and sparse areas. This patchy trend is more obvious in the hippocampus and striatum as described in the next sections. Meanwhile, it is noteworthy that superficial layers, especially layer 1, show patchy (though less pronounced) patterns. Of note, experience-dependent synaptic plasticity has been observed in the adult brain in layer 1 (Trachtenberg et al. 2002).

The cortical white matter—the corpus callosum—shows glycogen immunoreactivity, albeit at lower levels than the gray matter. We present both IV and ESG immunoreactivity in the corpus callosum and hippocampal alveus in Fig. 6. As analyzed

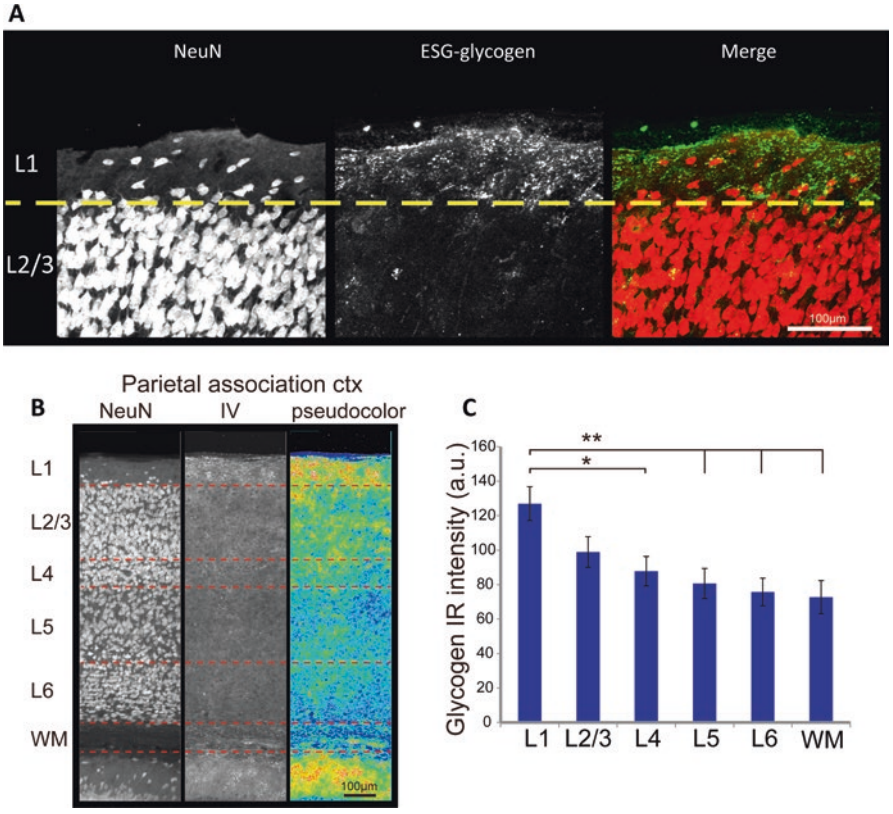

Fig. 6 Layer-dependent glycogen distribution in the mouse cortex. (**a**) ESG glycogen immunohistochemistry shows an enriched condensation of glycogen in layer 1. (**b** and **c**) IV glycogen immunohistochemistry shows a layer-dependent glycogen distribution pattern where glycogen signals are higher in superficial layers (reproduced from Oe et al. (2016))

by Oe et al. (2016), the majority of glycogen signals are detected in astrocytes. Oligodendrocytic localization of glycogen particles has been evaluated in myelin basic protein-positive structures, showing an order of magnitude smaller signal strengths, which may be signal leak from white matter astrocytes due to the resolution limit of confocal microscopy. Indeed, published electron microscopic observations have reported lack of glycogen in cortical and callosal oligodendrocytes (Caley and Maxwell 1968; Mori and Leblond 1969) while callosal astrocytes store abundant amounts of glycogen (Mori and Leblond 1969). However, in peripheral nerves, myelin-forming Schwann cells have been reported to store glycogen (Brown et al. 2012). The functional significance of white matter glycogen has been established as energy source mobilized during energy-scarce conditions (e.g., anoxia and hypoglycemia) in the optic nerve (Brown et al. 2003; Wender et al. 2000).

5.2 Hippocampus

The hippocampus is an allocortical structure known for its critical role in episodic memory formation. Hippocampal glycogenolysis has been shown to be crucial for long-term plasticity and consolidation of memory in the recent decade by pharmacological inhibition of glycogen phosphorylase using 1,4-dideoxy-1,4-imino-d-arabinitol (Newman et al. 2011; Suzuki et al. 2011). Glycogenolysis and the downstream metabolism have been suggested to be promoted by the beta-2 noradrenergic receptor (Gao et al. 2016). Hippocampal glycogen levels decrease by prolonged exhaustive exercises, during which multiple major monoamine levels (dopamine, noradrenaline, serotonin) are elevated (Matsui et al. 2011). These monoamines are released by volume transmission and activate astrocytic metabotropic pathways via respective G protein-coupled receptors (for a review, Hirase et al. 2014). Of note, recent papers suggest co-release of noradrenaline and dopamine from classical noradrenergic fibers originating in the locus coeruleus (Kempadoo et al. 2016; Takeuchi et al. 2016). Given the involvement of glycogen in synaptic plasticity and memory consolidation, its distribution in the hippocampus is an important topic and gains further insights into how glycogen metabolism is organized in behaving animals.

The hippocampus is a glycogen-rich structure and the IV antibody labels both the hippocampus proper and dentate gyrus intensely. Glycogen amount has a layer dependence. Principal cell body layers are low in glycogen content most likely due to the highly condensed neuronal somatic presence and hence relatively scarce astrocytic somata and processes (Ogata and Kosaka 2002). By contrast, layers populated by principal cell dendrites have high glycogen levels. These layers include strata oriens, radiatum, lucidum (CA3 only), and lacunosum-moleculare of the hippocampus proper; stratum moleculare and hilus of the dentate gyrus. Glycogen distribution appears seamless across CA1, CA2, and CA3. There is an impression that the CA3 stratum lucidum has subtly lower glycogen signals than other neuropil layers.

Remarkably, the ESG antibody labels the hilus more intensely than all other layers. The functional significance of high glycogen signals in the hilus remains elusive, yet there is an intriguing coincidence that the hilus receives the most intense noradrenergic innervation amongst all hippocampal layers (Loy et al. 1980), hinting at a noradrenergic drive of glycogen metabolism. The hilus is also known as the polymorphic layer and contains unmyelinated axons from dentate granule cells and various types of GABAergic interneurons. Hilar interneurons have been reported to discharge at high rates during dentate spikes—spontaneous, massive, synchronized neuronal activities originating in the dentate gyrus (Bragin et al. 1995). Moreover, neurogenesis continues to occur in the subgranular zone in adulthood, making the hilus subject to axonal proliferation which accompanies ATP-dependent actin polymerization. These features are suggestive of high energy demands in the hilus, and glycogen storage may guarantee sustained energy supply.

Similar to the cortex, IV antibody shows high-intensity punctate patterns with smooth low-intensity signals in the cytosol, the former presumably labeling beta glycogen aggregates. ESG glycogen immunohistochemistry shows a striking pattern in young adult mice in that large puncta are distributed in a "patchy" pattern consisting of puncta-busy and puncta-sparse areas (Fig. 7). The patchy patterns are present in the neuropil areas of the hippocampus proper and dentate gyrus, while patchy patterns are more obvious in the hippocampus proper. The patches are delineated by the morphology of individual astrocytes: there are astrocytes with dense ESG-labeled glycogen puncta and another population of astrocytes devoid of ESG labeling (Oe et al. 2016). Whether these glycogen-puncta-rich and -poor astrocytes comprise two molecularly distinct astrocyte populations or the glycogen storage difference is induced by local environmental factors is not known. Interestingly, the patchy glycogen pattern generally disappears in aged mice. IV glycogen immunohistochemistry shows more uniform distribution in the hippocampus of aged mice, whereas ESG glycogen immunohistochemical signals become low with sporadic high-signal spots reminiscent of polyglucosan bodies. Such alterations in glycogen IHC signals in the aged mouse brain could reflect the known aging-induced increase in *corpora amylacea*.

5.3 Striatum

The striatum, a major subcortical structure in rodents, is known for its function in motor executive functions, reward cognition, reinforcement learning, and motivational salience. Two major afferents to the striatum are the glutamatergic and dopaminergic projections from the cortex and substantia nigra, respectively. The striatum is distinct from other forebrain structures in that the principal cells are GABAergic. In fact, GABAergic medial spiny neurons represent >95% of the neuronal population. Medial spiny neurons are classified into D1 and D2 dopamine receptor-dominant types, which form the direct and indirect afferent pathways, respectively. There does not seem to be a strict spatial organization of D1 and D2 medial spiny neurons and they

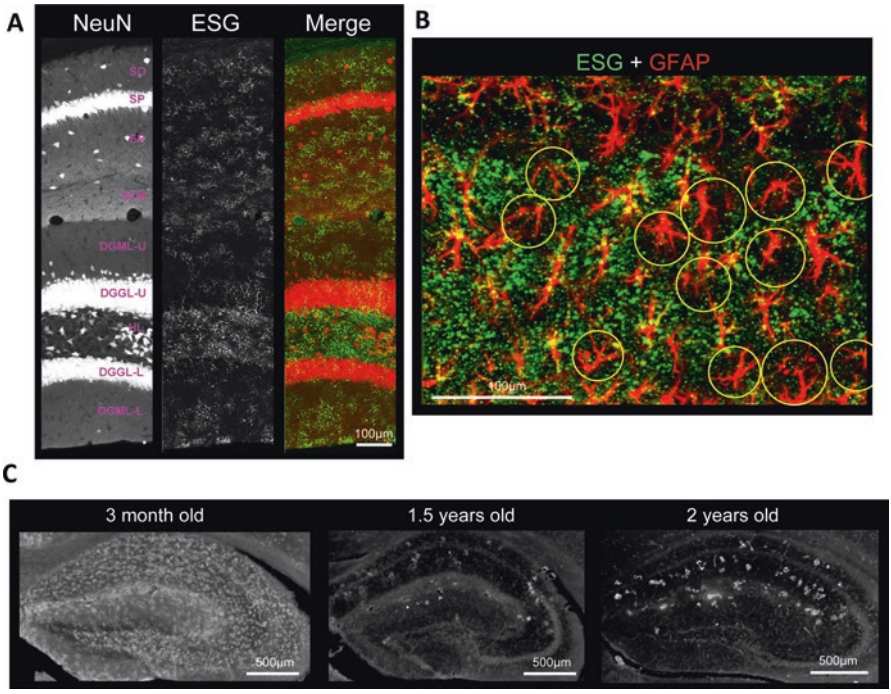

Fig. 7 Patchy glycogen distribution in the mouse hippocampus. (**a**) ESG glycogen immunohistochemistry across hippocampal layers. ESG signals are clustered in patches in dendritic layers (SO, SP, SR, SLM) of dorsal CA1. SO: stratum oriens, SP: stratum pyramidale, SR: stratum radiatum, SLM: stratum lacunosum-moleculare, DGML-U/L: dentate gyrus molecular layer upper/lower blade, DGGL-U/L: dentate gyrus granular layer upper/lower blade, HL hilus. (**b**) Double immunohistochemistry of ESG-labeled glycogen (green) and GFAP (red) shows that patchy glycogen distribution is organized by individual astrocytes. Yellow circles indicate astrocytes that comprise off-patch areas. The sample is from CA1 SP (upper ~15%) and SR (lower ~85%). (**c**) Patchy distribution disappear in aged mice and sporadic high-signal-intensity spots are evident. Reproduced from Oe et al. (2016) with modifications

appear to be homogeneously intermingled. Striatal cytoarchitecture is characterized by the frequent presence of myelinated fiber bundles of cortical and thalamic origins that pierce through the neuropil in stripes. In addition to the white/gray matter segregation, the striatum has histologically identified blobs (e.g., by μ-opioid receptor expression) called the striosomes (also known as the "patches," but here we avoid this term—not to be confused with the patchy glycogen distribution), while the remaining part is referred to as the matrix. In mice coronal sections, the striosomes appear as irregularly shaped areas of diagonal size 100–300 μm and are 300–600 μm apart.

Despite the vastly different cytoarchitecture, mouse striatal glycogen distribution share similar patterns to that of hippocampus proper neuropil. The neuropil is labeled well by IV and ESG antibodies, whereas the fiber bundle white matter yields relatively low glycogen signals. Remarkably, patchy glycogen puncta distributions

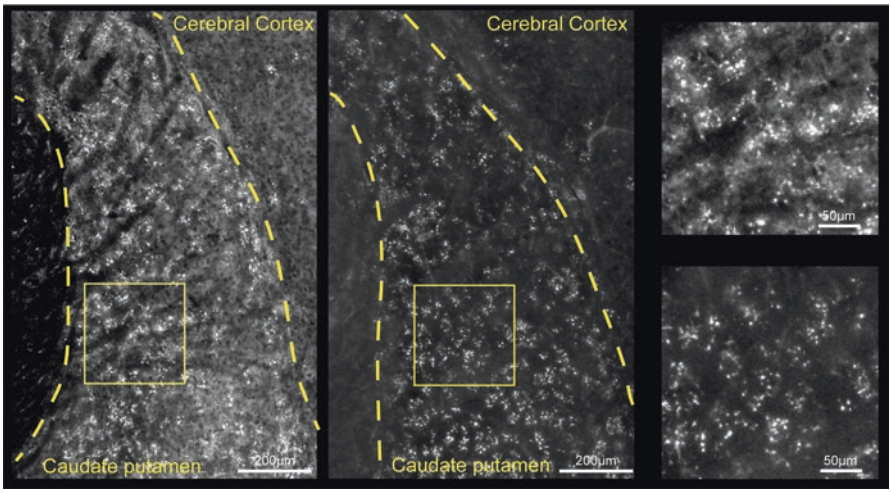

Fig. 8 Glycogen distribution in the striatum. IV (left) and ESG (center) glycogen immunohistochemistry in the mouse striatum (caudate putamen). Dashed lines indicate the borders with the internal capsule (to the left, basal ganglia white matter) and cerebral cortex (to the right). IV glycogen immunohistochemistry shows that striatal fiber bundles (white matter) are devoid of glycogen signals. Patchy patterns are observable with ESG signals. Areas marked by yellow squares are magnified in the right panels

are observed throughout the extent of striatal neuropil. As in the hippocampus, the patchy distribution is organized by intermingled distribution of ESG-immunoreactive and relatively ESG-free astrocytes (Fig. 8). Striatal patchy patterns are organized with a patch size of 50–150 μm, which is smaller than striosomes. Whether the glycogen patches are related to the distribution of D1 and D2 medial spiny neurons remains to be addressed. However, since medial spiny neurons are fairly densely distributed (< 50 μm apart) and their dendrites do not distinguish territories, heterogeneous astrocytic glycogen amounts are not deemed to be defined by proximity to D1 or D2 medial spiny neurons. A recent study suggested that striatal astrocytes are functionally classified into subtypes depending on their preference to signal to either medial spiny neuron subtype (Martin et al. 2015). It remains possible that this astrocytic diversity is related to the patchy glycogen pattern.

5.4 Olfactory Bulb

The olfactory bulb is a specialized allocortical structure that processes odor information. It is stratified with seven cytoarchitecturally distinct layers, namely: olfactory nerve layer; glomerular layer, external plexiform layer; mitral cell layer; internal plexiform layer; granule cell layer; and subependymal layer. It receives projections from the olfactory epithelium that terminate in the glomerular layer via the olfactory nerve layer.

The principal cells of the olfactory bulb are mitral and tufted cells whose dendrites comprise glomeruli, the characteristic neuropil-rich structures that receive olfactory nerve projections. Each glomerulus represents an elementary feature of a smell, and the combination of glomerular output is considered to encode complex olfactory information that is passed onto the olfactory cortex.

Overall, the olfactory bulb glycogen signal level is comparable to that in the cerebral cortex according to the strength of IV signal. IV glycogen immunohistochemistry delineates cytoarchitectural characteristics of the olfactory bulb, which is an indication that the storage of glycogen depends on cell type. Evidently, the mitral cell layer is virtually devoid of glycogen signals and glomeruli are outlined with a strip of low signal intensity area that coincide with the territory of juxtaglomerular (aka periglomerular) neurons. The granule cell layer is generally low in glycogen levels except for a mesh-like structure presumably representing astrocytic syncytium. Unlike the hippocampus, patchy patterns are not observed in the neuropil of external and internal plexiform layers or within a glomerulus. Glomeruli are easily distinguishable because of their relatively high glycogen content compared to external plexiform layer neuropil (Fig. 9). These relative glycogen levels are analogous to the expression of glycogen phosphorylase activity observed in the young rat (Coopersmith and Leon 1987). The olfactory bulb receives heavy neuromodulatory projections including noradrenergic, serotonergic, and cholinergic fibers. In addition, some 10% of juxtaglomerular neurons are dopaminergic. Noradrenergic activity-induced glycogenolysis in the rat olfactory bulb has been demonstrated using a biochemical glycogen assay (Coopersmith and Leon 1995). According to this work, beta adrenergic receptor activation is the main trigger of glycogenolysis while alpha adrenergic receptor (presumably alpha-1) activation becomes gradually dominant as the rat matures.

5.5 Non-forebrain Areas

Outside the forebrain, the cerebellum and brain stem are high in glycogen storage. Neuronal localization of glycogen in non-forebrain areas has been reported previously. For example, in the facial nucleus of the rat brain stem, glycogen immunohistochemical puncta are mainly found in motor neurons as identified by the expression of NR3B (NMDA receptor subunit 3B) cells (Takezawa et al. 2015). The same study also reports relative scarceness of astrocytic glycogen, although we shall note that glycogen immunohistochemistry was performed on perfusion-fixed brains. Also, we find that brain stem neurons with large somata (>30 μm diameter) tend to accumulate visible amounts of glycogen puncta.

Most literature agrees that the cerebellum is a rich, if not the richest, site of glycogen storage. The cerebellar cortex consists of three layers: the molecular, Purkinje, and granular layer. The Purkinje layer is the cell body layer of Purkinje cells (the GABAergic principal output cells) and Bergmann glia that enwrap the synapses of Purkinje cells in full (Grosche et al. 1999). Purkinje cells' dendrites are formed in

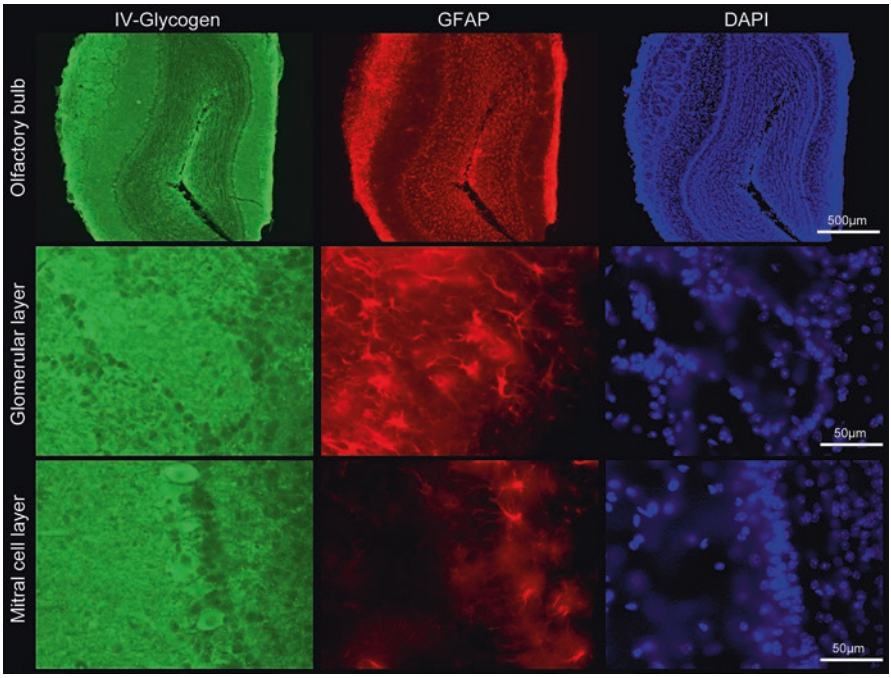

Fig. 9 Glycogen distribution in the olfactory bulb. IV glycogen immunohistochemistry (left) was performed together with GFAP immunohistochemistry (center) and DAPI staining (right). Glomerular and mitral cell layers are magnified in middle and bottom panels, respectively (the olfactory nerve layer is to the left). Glycogen distributions show a characteristic layer-dependent pattern. Glomeruli show high glycogen signals. Whereas periglomerular somata are low in glycogen signal. Mitral cell somata are low in glycogen, however, a population of neuron-like somata show visible green fluorescence

the molecular layer which is superficial to the Purkinje layer. A Purkinje cell has up to 200,000 spines that form synapses with parallel fibers (Napper and Harvey 1988), projecting axons from granule cells that run perpendicularly to the Purkinje cell dendrite plane. In addition, each Purkinje cell is innervated by a climbing fiber which provides powerful excitatory input. Finally, the granular layers are where glutamatergic granule cell bodies are located. Instead of Bergmann glia, the granular layer is populated with so-called velate astrocytes, a kind of protoplasmic astrocytes that ensheath granule cells. Glycogen immunohistochemistry reveals that the molecular layer of the cerebellar cortex has the most intensive glycogen immunohistochemical signals in the mouse brain. Moreover, the granular layer shows scattered distribution of punctate glycogen signals, showing signs of velate astrocytic localization. Bergmann glia accumulate glycogen as evidenced by IV and ESG signals from relatively small somata located in between Purkinje cells. Further characterization of glycogen distribution in the cerebellar cortex is desired and we are currently conducting a more detailed examination of cerebellar glycogen distribution in the mouse.

6 Concluding Remarks

In this chapter, we have described murine brain glycogen distribution according to glycogen immunohistochemistry. Glycogen immunohistochemistry allowed the assessment of regional variability. As a result, we were able to find layer differences in cortical structures and patchy patterns in the hippocampus, striatum, and to a smaller extent, superficial layers of the cortex.

An important issue to remember is that glycogen is a dynamic molecule whose size depends on the metabolic state, which is most likely governed by brain states. Brain glycogen immunohistochemistry data presented here and in Oe et al. (2016) are from mice sacrificed at the end of the light phase of 12/12 h light/dark housing condition. Glycogen distribution may differ in animals prepared at different hours, behavioral conditions, and levels of maturity. In fact, we found that the patchy ESG-labeled glycogen patterns disappear in aged mice. Instead, the ESG antibody labels much larger clots, presumably polyglucosan bodies, that appear frequently (5–30 per hippocampal slice depending on age) in the hippocampus. A previous report suggested that such polyglucosan accumulation is observed in neurons (Sinadinos et al. 2014). More recently, proteomic analyses in the hippocampus revealed a shift of glycogen metabolism enzymes' expression from astrocytes to neurons as mice age (Drulis-Fajdasz et al. 2018). Such a change in metabolism may underlie the disappearance of patchy pattern in aged mice, while functional significances of patchy glycogen distribution remain elusive. Another situation where glycogen storage is altered in astrocytes is inflammation (Shimizu and Hamuro 1958). An electron microscopy study reported that astrocytes accumulate higher amounts of glycogen after radioactive irradiation (Maxwell and Kruger 1965). Further investigations are needed to identify the dynamic nature of brain glycogen distribution in health and disease.

Acknowledgements This work was supported by the RIKEN Brain Science Institute, KAKENHI grants (26117520, 16H01888, 18H05150), and HFSP (RGP0036/2014). We thank members of the laboratory for comments on earlier versions of the manuscript. The authors declare no competing financial interests. SA is supported by the RIKEN IPA program.

References

Anton-Sanchez L, Bielza C, Merchán-Pérez A, Rodríguez J-R, DeFelipe J, Larrañaga P (2014) Three-dimensional distribution of cortical synapses: a replicated point pattern-based analysis. Front Neuroanat 8:85

Baba O (1993) Production of monoclonal antibody that recognizes glycogen and its application for immunohistochemistry. Kokubyo Gakkai Zasshi 60:264–287

Bragin A, Jando G, Nadasdy Z, van Landeghem M, Buzsaki G (1995) Dentate EEG spikes and associated interneuronal population bursts in the hippocampal Hilar region of the rat. J Neurophysiol 73:1691–1705

Brown AM, Tekkök SB, Ransom BR (2003) Glycogen regulation and functional role in mouse white matter. J Physiol 549:501–512
Brown AM, Evans RD, Black J, Ransom BR (2012) Schwann cell glycogen selectively supports myelinated axon function. Ann Neurol 72:406–418
Caley DW, Maxwell DS (1968) An electron microscopic study of the neuroglia during postnatal development of the rat cerebrum. J Comp Neurol 133:45–69
Calì C, Baghabra J, Boges DJ, Holst GR, Kreshuk A, Hamprecht FA, Srinivasan M, Lehväslaiho H, Magistretti PJ (2016) Three-dimensional immersive virtual reality for studying cellular compartments in 3D models from EM preparations of neural tissues. J Comp Neurol 524:23–38
Cataldo AM, Broadwell RD (1986) Cytochemical identification of cerebral glycogen and glucose-6-phosphatase activity under normal and experimental conditions. II. Choroid plexus and ependymal epithelia, endothelia and pericytes. J Neurocytol 15:511–524
Chandrasekaran S, Navlakha S, Audette NJ, McCreary DD, Suhan J, Bar-Joseph Z, Barth AL (2015) Unbiased, high-throughput electron microscopy analysis of experience-dependent synaptic changes in the neocortex. J Neurosci 35:16450–16462
Choi HB, Gordon GRJ, Zhou N, Tai C, Rungta RL, Martinez J, Milner TA, Ryu JK, McLarnon JG, Tresguerres M, Levin LR, Buck J, MacVicar BA (2012) Metabolic communication between astrocytes and neurons via bicarbonate-responsive soluble adenylyl cyclase. Neuron 75:1094–1104
Cline GW, Petersen KF, Krssak M, Shen J, Hundal RS, Trajanoski Z, Inzucchi S, Dresner A, Rothman DL, Shulman GI (1999) Impaired glucose transport as a cause of decreased insulin-stimulated muscle glycogen synthesis in type 2 diabetes. N Engl J Med 341:240–246
Coopersmith R, Leon M (1987) Glycogen phosphorylase activity in the olfactory bulb of the young rat. J Comp Neurol 261:148–154
Coopersmith R, Leon M (1995) Olfactory bulb glycogen metabolism: noradrenergic modulation in the young rat. Brain Res 674:230–237
DeFelipe J, Alonso-Nanclares L, Arellano JI (2002) Microstructure of the neocortex: comparative aspects. J Neurocytol 31:299–316
Drulis-Fajdasz D, Gizak A, Wójtowicz T, Wiśniewski JR, Rakus D (2018) Aging-associated changes in hippocampal glycogen metabolism in mice. Evidence for and against astrocyte-to-neuron lactate shuttle. Glia 66:1481–1495
Fiala JC, Kirov SA, Feinberg MD, Petrak LJ, George P, Goddard CA, Harris KM (2003) Timing of neuronal and glial ultrastructure disruption during brain slice preparation and recovery in vitro. J Comp Neurol 465:90–103
Gao V, Suzuki A, Magistretti PJ, Lengacher S, Pollonini G, Steinman MQ, Alberini CM (2016) Astrocytic β2-adrenergic receptors mediate hippocampal long-term memory consolidation. Proc Natl Acad Sci 113:8526–8531
Gibbs ME, Anderson DG, Hertz L (2006) Inhibition of glycogenolysis in astrocytes interrupts memory consolidation in young chickens. Glia 54:214–222
Grosche J, Matyash V, Moller T, Verkhratsky A, Reichenbach A, Kettenmann H (1999) Microdomains for neuron-glia interaction: parallel fiber signaling to Bergmann glial cells. Nat Neurosci 2:139–143
Hirase H, Iwai Y, Takata N, Shinohara Y, Mishima T (2014) Volume transmission signalling via astrocytes. Philos Trans R Soc B 369:20130604
Kempadoo KA, Mosharov EV, Choi SJ, Sulzer D, Kandel ER (2016) Dopamine release from the locus coeruleus to the dorsal hippocampus promotes spatial learning and memory. Proc Natl Acad Sci 113:14835–14840
Koizumi J (1974) Glycogen in the central nervous system. Prog Histochem Cytochem 6:1–37
Kong J, Shepel PN, Holden CP, Mackiewicz M, Pack AI, Geiger JD (2002) Brain glycogen decreases with increased periods of wakefulness: implications for homeostatic drive to sleep. J Neurosci 22:5581–5587
Loy R, Koziell DA, Lindsey JD, Moore RY (1980) Noradrenergic innervation of the adult rat hippocampal formation. J Comp Neurol 189:699–710

Magnusson I, Rothman DL, Katz LD, Shulman RG, Shulman GI (1992) Increased rate of gluconeogenesis in type II diabetes mellitus. A 13C nuclear magnetic resonance study. J Clin Invest 90:1323–1327

Martin R, Bajo-Graneras R, Moratalla R, Perea G, Araque A (2015) Circuit-specific signaling in astrocyte-neuron networks in basal ganglia pathways. Science 349:730–734

Matsui T, Soya S, Okamoto M, Ichitani Y, Kawanaka K, Soya H (2011) Brain glycogen decreases during prolonged exercise. J Physiol 589:3383–3393

Maxwell DS, Kruger L (1965) The fine structure of astrocytes in the cerebral cortex and their response to focal injury produced by heavy ionizing particles. J Cell Biol 25:141–157

Mori S, Leblond CP (1969) Electron microscopic features and proliferation of astrocytes in the corpus callosum of the rat. J Comp Neurol 137:197–225

Nakamura-Tsuruta S, Yasuda M, Nakamura T, Shinoda E, Furuyashiki T, Kakutani R, Takata H, Kato Y, Ashida H (2012) Comparative analysis of carbohydrate-binding specificities of two anti-glycogen monoclonal antibodies using ELISA and surface plasmon resonance. Carbohydr Res 350:49–54

Napper RMA, Harvey RJ (1988) Number of parallel fiber synapses on an individual Purkinje cell in the cerebellum of the rat. J Comp Neurol 274:168–177

Newman LA, Korol DL, Gold PE (2011) Lactate produced by glycogenolysis in astrocytes regulates memory processing. PLoS One 6:e28427

Obel LF, Müller MS, Walls AB, Sickmann HM, Bak LK, Waagepetersen HS, Schousboe A (2012) Brain glycogen-new perspectives on its metabolic function and regulation at the subcellular level. Front Neuroenerg 4:3

Oe Y, Baba O, Ashida H, Nakamura KC, Hirase H (2016) Glycogen distribution in the microwave-fixed mouse brain reveals heterogeneous astrocytic patterns. Glia 64:1532–1545

Ogata K, Kosaka T (2002) Structural and quantitative analysis of astrocytes in the mouse hippocampus. Neuroscience 113:221–233

Öz G, Henry PG, Seaquist ER, Gruetter R (2003) Direct, noninvasive measurement of brain glycogen metabolism in humans. Neurochem Int 43:323–329

Öz G, Seaquist ER, Kumar A, Criego AB, Benedict LE, Rao JP, Henry P-G, Van De Moortele P-F, Gruetter R (2007) Human brain glycogen content and metabolism: implications on its role in brain energy metabolism. Am J Physiol Metab 292:E946–E951

Palomero-Gallagher N, Zilles K (2017) Cortical layers: cyto-, myelo-, receptor- and synaptic architecture in human cortical areas. NeuroImage 197:716–741

Phelps CH (1972) Barbiturate-induced glycogen accumulation in brain. An electron microscopic study. Brain Res 39:225–234

Prats C, Graham TE, Shearer J (2018) The dynamic life of the glycogen granule. J Biol Chem 293(19):7089–7098

Raichle ME, Gusnard DA (2002) Appraising the brain's energy budget. Proc Natl Acad Sci U S A 99:10237–10239

Sagar SM, Sharp FR, Swanson RA (1987) The regional distribution of glycogen in rat brain fixed by microwave irradiation. Brain Res 417:172–174

Schuz A, Palm G (1989) Density of neurons and synapses in the cerebral cortex of the mouse. J Comp Neurol 286:442–455

Shimizu N, Hamuro Y (1958) Deposition of glycogen and changes in some enzymes in brain wounds. Nature 181:781–782

Sinadinos C, Valles-Ortega J, Boulan L, Solsona E, Tevy MF, Marquez M, Duran J, Lopez-Iglesias C, Calbó J, Blasco E, Pumarola M, Milán M, Guinovart JJ (2014) Neuronal glycogen synthesis contributes to physiological aging. Aging Cell 13:935–945

Sugiura Y, Honda K, Kajimura M, Suematsu M (2014) Visualization and quantification of cerebral metabolic fluxes of glucose in awake mice. Proteomics 14:829–838

Suzuki A, Stern SA, Bozdagi O, Huntley GW, Walker RH, Magistretti PJ, Alberini CM (2011) Astrocyte-neuron lactate transport is required for long-term memory formation. Cell 144:810–823

Swanson RA, Morton MM, Sagar SM, Sharp FR (1992) Sensory stimulation induces local cerebral glycogenolysis: demonstration by autoradiography. Neuroscience 51:451–461

Takado Y, Knott G, Humbel BM, Escrig S, Masoodi M, Meibom A, Comment A (2015) Imaging liver and brain glycogen metabolism at the nanometer scale. Nanomedicine 11:239–245

Takano T, He W, Han X, Wang F, Xu Q, Wang X, Oberheim Bush NA, Cruz N, Dienel GA, Nedergaard M (2014) Rapid manifestation of reactive astrogliosis in acute hippocampal brain slices. Glia 62:78–95

Takeuchi T, Duszkiewicz AJ, Sonneborn A, Spooner PA, Yamasaki M, Watanabe M, Smith CC, Fernández G, Deisseroth K, Greene RW, Morris RGM (2016) Locus coeruleus and dopaminergic consolidation of everyday memory. Nature 537:357–362

Takezawa Y, Baba O, Kohsaka S, Nakajima K (2015) Accumulation of glycogen in axotomized adult rat facial motoneurons. J Neurosci Res 93:913–921

Testoni G, Duran J, García-Rocha M, Vilaplana F, Serrano AL, Sebastián D, López-Soldado I, Sullivan MA, Slebe F, Vilaseca M, Muñoz-Cánoves P, Guinovart JJ (2017) Lack of Glycogenin causes glycogen accumulation and muscle function impairment. Cell Metab 26:256–266.e4

Trachtenberg JT, Chen BE, Knott GW, Feng G, Sanes JR, Welker E, Svoboda K (2002) Long-term in vivo imaging of experience-dependent synaptic plasticity in adult cortex. Nature 420:788–794

Wang J, Tu J, Cao B, Mu L, Yang X, Cong M, Ramkrishnan AS, Chan RHM, Wang L, Li Y (2017) Astrocytic l -lactate signaling facilitates amygdala-anterior cingulate cortex synchrony and decision making in rats. Cell Rep 21:2407–2418

Wender R, Brown AM, Fern R, Swanson RA, Farrell K, Ransom BR (2000) Astrocytic glycogen influences axon function and survival during glucose deprivation in central white matter. J Neurosci 20:6804–6810

Wong-Riley M (1979) Changes in the visual system of monocularly sutured or enucleated cats demonstrable with cytochrome oxidase histochemistry. Brain Res 171:11–28

Wong-Riley MT, Welt C (1980) Histochemical changes in cytochrome oxidase of cortical barrels after vibrissal removal in neonatal and adult mice. Proc Natl Acad Sci U S A 77:2333–2337

Zhu X, Bergles DE, Nishiyama A (2007) NG2 cells generate both oligodendrocytes and gray matter astrocytes. Development 135:145–157